Avrupa Bilim ve Teknoloji Dergisi
Özel Sayı 24, S. 430-435, Nisan 2021

Araştırma Makalesi

www.ejosat.com ISSN:2148-2683

European Journal of Science and Technology
Special Issue 24, pp. 430-435, April 2021

Research Article

Variable Stiffness Woven Fabrics with Curved Advanced Fibers

Muhsin Gökhan Günay[1*], Taner Timarcı[2]

[1*] Akdeniz University, Faculty of Engineering, Departmant of Mechanical Engineering, Antalya, Turkey, (ORCID: 0000-0002-8895-1710), gmgunay@akdeniz.edu.tr
[2] Trakya University, Faculty of Engineering, Departmant of Mechanical Engineering, Edirne, Turkey, (ORCID: 0000-0003-3966-7614), tanert@trakya.edu.tr

(2nd International Conference on Access to Recent Advances in Engineering and Digitalization (ARACONF)-10–12 March 2021)

(**DOI:** 10.31590/ejosat.898542)

ATIF/REFERENCE: Günay, M.G., Timarcı, T. (2021). Variable Stiffness Woven Fabrics with Curved Advanced Fibers. *European Journal of Science and Technology*, (24), 430-435.

Abstract

A novel method for production of variable stiffness woven fabrics with curved advanced fibers is presented. A scalable concept design is introduced. Several variable stiffness fabrics are woven by the prototype loom. The weaving process and woven fabrics are examined. Two distinct regions of the fabric which are showing different behaviors are observed. Based on the two regions identified the curved fibers of the woven fabric are simplified and modeled as a three-dimensional unit mesh. Geometry variation of the curved fibers and stiffness variation of the woven fabrics are discussed for these two distinct regions by using the developed model.

Keywords: Woven fabric, Curved fiber, Variable stiffness, Yarn geometry, Composite.

Gelişmiş Eğrisel Fiberli Değişken Rijitlikli Dokunmuş Kumaşlar

Öz

Bu çalışmada eğrisel gelişmiş ipliklere sahip değişken rijitlikli dokuma kumaşların üretimi için yeni bir yöntem sunulmuştur. Ölçeklenebilir bir konsept tasarım tanıtılmıştır. Prototip dokuma tezgahı ile değişken rijitlikli kumaşlar dokunmuştur. Dokuma işlemi ve dokunan kumaşlar incelenmiştir. Kumaşlarda farklı davranışlar gösteren iki ayrı bölgenin olduğu gözlenmiştir. Belirlenen iki bölgeye dayanarak, dokuma kumaşın eğimli iplikleri basitleştirilmiş ve üç boyutlu birim yapı olarak modellenmiştir. Eğri ipliklerin geometri değişimi ve dokuma kumaşların rijitlik değişimi, geliştirilen model kullanılarak bu iki farklı bölge için tartışılmıştır.

Anahtar Kelimeler: Dokuma kumaş, Eğrisel elyaf, Değişken rijitlik, İplik geometrisi, Kompozit.

[*] Corresponding Author: gmgunay@akdeniz.edu.tr

1. Introduction

Composites reinforced by advanced fibers are widely used in practice, including the aerospace, automotive, sports and biomedical industry where the light weight and the high strength are important. The most of the advanced reinforcement fibers such as glass, carbon, and aramid have higher strength along its longitudinal axis relative to its transverse axis (Campbell, 2010). Conventionally composite structures are constructed as a stack of layers of the advanced fibers where fibers lay straight in their own plane. The mechanical properties of the composite structure can be controlled by changing the orientations the fibers in these layers. As fibers lay straight in their own plane, the stiffness of these layers depends only on the fiber orientations of each layer. The mechanical properties of the layered composite structures can be changed by varying the distance between fibers as Martin and Leissa (1990) expressed as well as by giving a curvilinear form to fibers in their own planes as Gürdal and Olmedo (1993) demonstrated in their article.

Theory of the variable stiffness plates and cylinders with curved fibers are vastly studied in the literature. One of the first studies on the topic can be counted as the works of Hyer et.al. (1991) where they used curvilinear fibers to increase buckling performance of a rectangular plate with a central hole. Gürdal et.al. (2008) also expressed that using curvilinear fibers on plate structures increases the buckling performance of the structure. Blom et.al. (2010) optimized composite cylinders under bending by tailoring stiffness properties in circumferential direction. The optimization of the path definitions of curved fibers to maximize fundamental eigenfrequency of conical shells is also investigated by Blom et.al. (2008). Zamani et.al. (2011) worked on thin-walled beams with bi-convex cross-section and utilized curvilinear fibers to optimize them. Recently, the authors of the present work, Günay and Timarcı presented a formulation for static analysis of thin walled composite beams with variable stiffness and thickness (Günay & Timarci, 2017) and investigated their stress distributions along the hoop direction (Günay & Timarcı, 2019).

There are several methods in the literature such as Automated Tape Laying (ATL), Automated Fiber Placement (AFP), Tow Shearing, Tow Steering and Tailored Fiber Placement (August et.al., 2014; Brooks & Martins, 2018; Crothers et.al., 1997; Dirk et.al., 2012; Kim et.al., 2014; Smith & Grant, 2006; Zhang et.al., 2020) to construct the variable stiffness composite layers or structures with curved fibers. Each of these methods have its own working principle and advantages but generally the placement or stitching of the tows is realized directly on the surface of the composite part by using a robotic arm. Beside these methods Ashir et al. (2020) and Lenz et al. (2016) used open reed weaving technique to locally reinforce fabrics with advanced fibers where the orientation of the fibers can be tailored.

In this study a novel method to weave the variable stiffness fabrics having the curvilinear fibers is presented. A generic scalable concept design is proposed for the application of the method. Based on the concept design an automated prototype loom is constructed. Several variable stiffness fabrics are woven by use of this prototype loom. Three-dimensional geometry of the woven fabrics is investigated and modeled by using a unit mesh.

2. Concept Loom Design

On a conventional loom, which is also vastly used in composite industry, the fabrics are weaved by using a straight reed in which weft and warp yarns become perpendicular to each other. In the proposed method the working principle of a conventional loom is adopted to weave fabrics with curved fibers by using a curved reed instead of a conventional straight reed. The blades of the curved reed are moved forward or backward to follow a specific curved path so that the angle between the warp and weft yarns can be changed accordingly.

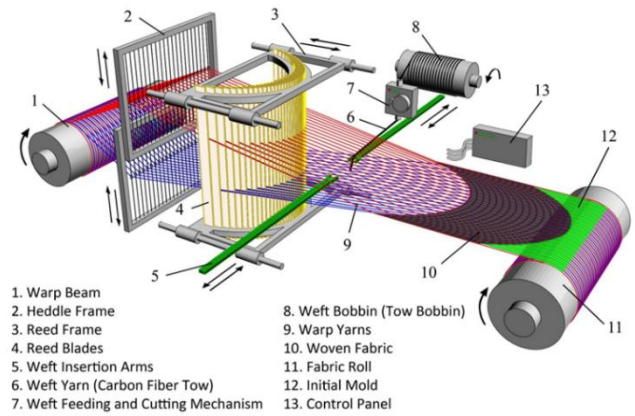

Fig.1. Main parts of concept loom.

The main components of the concept design of the proposed method and constructed prototype loom are presented in Fig.1 and Fig.2 respectively.

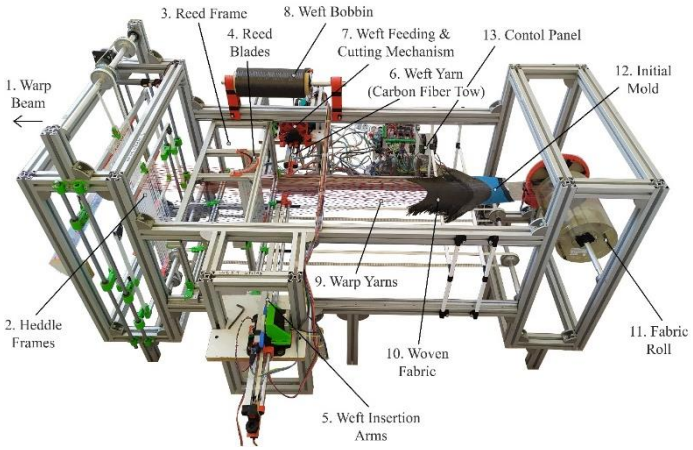

Fig. 2. Prototype loom.

The final curved shape of the weft yarns depends on the curved reed and the initial mold. The initial mold is prepared in a way to complement the curved reed by using the same curved path of the reed. The initial mold is actually a flexible plastic or cardboard plate placed between the warps yarns and fixed to them. It helps to give their curved shape to the weft yarns at the start of weaving. As the weft yarns get their curved shape, the angle between the weft and warp yarns varies along the width of the fabric. In the case of use of an advanced fiber which has a greater axial strength than its transverse strength (like carbon fiber, aramid fiber, glass fiber, etc.) as weft yarn, the woven fabric will have a variable stiffness depending on the curved path of the weft yarns.

In Fig.3 conventional straight reed, curved reed and initial mold is presented. As seen in Fig.3 placing the reed blades on the curved path creates a distance between anterior and posterior blades, while in a conventional reed all blades align on a straight row. Thus, curved reed design needs a longer stroke to pass completely the weft insertion arms while a pretty short stroke is enough for a conventional reed. The stroke length needed for the curved reed depends on the shape of the desired curved path and width of the woven fabric.

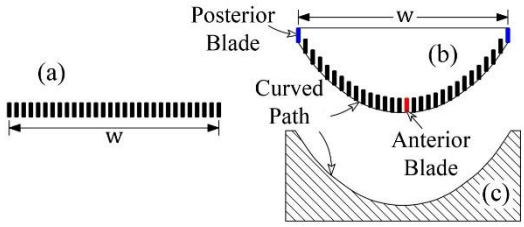

Fig.3. Conventional straight reed (a), curved reed (b) and initial mold (c).

Increasing the width of the woven fabric and the distance between anterior and posterior points of the curved path may also increase the needed stroke length of the heddle frames. When the heddle frames are apart, the distance between the frames are required to be long enough to create an enough triangular space between the anterior reed blade and warp yarns, where the weft insertion arms pass through.

3. Results and Discussion

3.1. Analysis of Woven Fabrics

Several variable stiffness fabrics are weaved with the constructed prototype loom by using carbon fiber weft yarns. Thin polyester sewing strings which have 24 tex number are used as warp yarns for all fabrics. The distance between two warp yarns (s) is set to 2.5 mm and each warp yarn is tensioned with approximately 750 N axial force. The woven fabrics weaved with a straight reed and a curved reed are given in Figs.4(a) and 4(b) respectively.

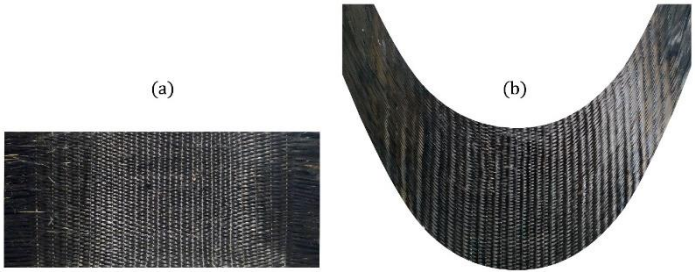

Fig.4. Woven fabrics weaved with a straight reed (a) and with a curved reed (b).

As seen from Fig.3 the proposed concept of the curved reed is able to weave fabrics with curved fibers successfully. It is seen that as the tension of the warp yarns are kept high enough the curved fibers keep their shape during the weaving process. Nevertheless, the fabric tends to lose its form at the open sides when the angle between the warp yarn and the weft yarn reduces under 15^o. As a limitation of the proposed method it is not feasible to place weft yarns between warp yarns with very small orientation angles especially when the angle between yarns reduces under 10^o. In this case some of the warp yarns can be replaced with the advanced fiber instead of the thin sewing strings. Consequently, these warp yarns can serve as a reinforcement fiber with 0^o orientation.

Maintaining the curved shape of the fibers until the usage of the woven fabric is very important as the external contacts may deform the fabric. This can be solved by pre-impregnating the woven fabrics and storing them as pre-pregs by use of solution impregnation, film impregnation or similar methods (Bai, 2013) especially for large scale productions.

3.2. Unit mesh model

When the weaving process of the fabric is investigated in detail it is observed that the weft yarns show two distinct behavior at two different regions of the fabric. The first and second regions are called as region-A and region-B and they are shown in Fig.5. The region-A locates between the warp yarns where the weft yarns touch each other whereas the region-B is identified where weft yarns pass over or under the warp yarns.

As seen from Fig.5 there are empty spaces around the following weft yarns at region-B while the weft yarns are densely packed at region-A. Presence or absence of the empty space around the weft yarns defines the behavior of the weft yarns when they are weaved by the curved reed. To model the behavior of these two regions and to acquire final geometry of the woven fabric the weft yarns are simplified and represented with a three-dimensional unit mesh.

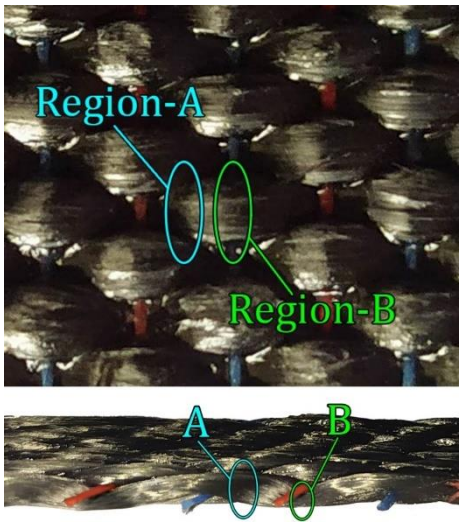

Fig.5. Region-A and region-B.

The unit mesh covers the section of the weft yarns from the region-A to region-B and it is constructed by 14 vertices as shown in Fig.6. The xyz cartesian coordinate system is used in analysis by placing the warp yarns along y-axis and the thickness along z-axis.

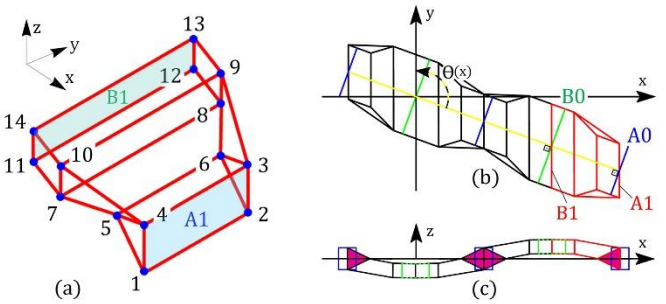

Fig.6. Unit mesh (a), top (b) and side (c) view of four joined units.

As seen in Fig.6 by aligning and repeating the unit mesh whole weft yarn can be modelled in three dimensions. The yellow line which is passing in the middle of the unit mesh shows the yarn orientation which is measured counter clockwise from yellow line to y-axis. Orientation of each unit mesh varies depended on the curved path of the weft yarns. As all weft yarns have same curved path they can be accepted as shifted copies of each other along the y-axis. Thus, their geometry and properties are constant along y-axis but variable along x-axis depended on the curved path of the weft yarns.

While deriving equations it is accepted that the cross-sectional area which is perpendicular to the orientation will be constant all over the weft yarn before and after weaving. The cross-sections of the weft yarns which are perpendicular to the orientation at the regions-A and B are called as cross-section A0 and B0 respectively to further use in calculations. As accepted, A0 and B0 both have equal areas but their dimensions may be different.

The rectangle which is covered by the first four vertices (1,2,3,4) of the unit mesh is called as rectangle-A1 and similarly the rectangle covered by the last four vertices (11,12,13,14) of the unit mesh is named as rectangle B1 as presented in Fig.6. By definition, even if the orientation of the unit mesh varies, the rectangles A1 and B1 will always stay parallel to the y-z plane. Coordinates of the vertices defining rectangles A1 and B1 are found by projecting the corner points of cross-sections A0 and B0 along the orientation to the planes which are parallel to the y-z plane and passing through the centers of A0 and B0 as given below. As A1 and B1 are projection of A0 and B0 respectively the height of A1 will be equal to the height of A0. Similarly, the heights of B1 and B0 will be equal.

It is observed that the weft yarns at region-A get their curved shape by shearing as they are pushed by the curved reed. When the weft yarns are forced to shear the perpendicular distance between two following weft yarns at region-A, which is the width of A0, decreases. And the height of A0 increases to keep the cross-sectional are constant as accepted. If the height of A0 at $\theta(x) = 90^o$, where the weft and warps yarns are perpendicular to each other, is chosen as reference the variation of $h_{A0}(x)$ can be calculated as given in Eq.1. A similar relation is also expressed in tow shearing method (Kim et al., 2012; Kim et al., 2014).

$$h_A(x) = \frac{h_{A,ref}}{\sin(\theta(x))} \quad (1)$$

The width of A0 can be found by dividing the cross-sectional area to the height of A0 as given below;

$$w_{A0}(x) = \frac{A}{h_A(x)} \quad (2)$$

The width of A1 (w_{A1}), which can be measured from fabric, is constant all over the fabric as the weft yarns are shifted copies of each other along y-axis and they are densely packed at region-A.

When region-B is investigated, it is seen that the weft yarns tend to spread to the empty spaces while they are passing under and over warp yarns. Because of this spreading behavior the width of B0 (w_{B0}) will be wider than the width of A0 (w_{A0}). The ratio of (w_{A0}) to (w_{B0}) at $\theta(x) = 90^o$ is called as "the width ratio" and shown by C_1. The width of A0 (w_{A0}) and the width of B0 (w_{B0}) can be directly measured from the woven fabric and the width ratio C_1 can be calculated as;

$$C_1 = \frac{w_{A0}}{w_{B0}}\Big|_{\theta(x)=90^o} \quad (3)$$

Then the height of B0 at $\theta(x) = 90^o$ which is called as ($h_{B,ref}$) can be calculated by using the width ratio C_1 as;

$$h_{B,ref} = C_1 . h_{A,ref} \quad (4)$$

Because of both shearing and spreading behavior of the weft yarns at region-B the height of B0 ($h_{B0}(x)$) is modelled by modifying Eq.1 with parameter C_2 as presented in Eq.5. The parameter C_2, which is called as "the shear factor", defines how much the area B0 shears or spreads as the orientation varies.

$$h_B(x) = h_{B,ref}\left(1 + C_2\left(\frac{1}{\sin(\theta(x))} - 1\right)\right) \quad (5)$$

The shear factor C_2 ranges from 0 to 1. If C_2 is chosen as zero B0 does not get effected from shearing and it rotates freely by keeping its dimensions. If C_2 is chosen as one B0 totally gets affected from shearing and the weft yarns do not spread. If C_2 is chosen between zero and one the weft yarns at region-B both shear and spread. It is seen that C_2 can depend on the yarn material used and also the pressure applied to the weft yarns while weaving. For investigated carbon fiber fabrics C_2 is found as 0.5 by trying different values and by comparing the calculated and measured values.

The variation of the width of B0 ($w_{B0}(x)$) can simply be calculated by dividing cross-sectional area (A) to $h_{B0}(x)$ as given below.

$$w_{B0}(x) = \frac{A}{h_{B0}(x)} \quad (6)$$

Then the width of B1 ($w_{B1}(x)$) can be calculated by projecting B0 to B1 as given in Eq.7.

$$w_{B1}(x) = \frac{w_{B0}(x)}{\sin(\theta(x))} \quad (7)$$

The spreading of the fibers along y-direction at region-B has a ceiling limit of ($2w_{A1}$) which is the maximum space the weft yarns can spread. While calculating the height of region-B this ceiling limit must be considered. Eq.5 will not be valid anymore if the $w_{B1}(x)$ value calculated by Eq.7 exceeds the ceiling limit of ($2w_{A1}$). In this case, the height of region-B must be calculated by using Eq.8 given below and depended values must be updated.

$$h_B(x) = \frac{A}{2w_{A1}.\sin(\theta(x))} \; if \; w_{B1}(x) \geq 2w_{A1} \quad (8)$$

The coordinates of the vertices of the unit mesh, which are representing region-A and region-B, are expressed as given below.

$$v_1 = \left[\frac{s}{2}, \frac{-w_{A1}}{2} + \frac{s}{2}\cot(\theta(x)), \frac{-h_A(x)}{2}\right] \quad (9a)$$

$$v_2 = \left[\frac{s}{2}, \frac{w_{A1}}{2} + \frac{s}{2}\cot(\theta(x)), \frac{-h_A(x)}{2}\right] \quad (9b)$$

$$v_3 = \left[\frac{s}{2}, \frac{w_{A1}}{2} + \frac{s}{2}\cot(\theta(x)), \frac{h_A(x)}{2}\right] \quad (9c)$$

$$v_4 = \left[\frac{s}{2}, \frac{-w_{A1}}{2} + \frac{s}{2}\cot(\theta(x)), \frac{h_A(x)}{2}\right] \quad (9d)$$

$$v_{11} = \left[0, \frac{-w_{B1}(x)}{2}, e\right] \quad (10a)$$

$$v_{12} = \left[0, \frac{w_{B1}(x)}{2}, e\right] \quad (10b)$$

$$v_{13} = \left[0, \frac{w_{B1}(x)}{2}, e + h_B(x)\right] \quad (10c)$$

$$v_{14} = \left[0, \frac{-w_{B1}(x)}{2}, e + h_B(x)\right] \quad (10d)$$

where (s) is the distance between two warp yarns and (e) is the eccentricity from x-y plane. Other vertices of the unit mesh are defined to mimic the translation from region-A to region-B as presented below.

$$v_5 = \left[\frac{s}{3} - s_1, \frac{-w_{A1}}{2} + \left(\frac{s}{3} - s_1\right)\cot(\theta(x)), 0\right] \quad (11a)$$

$$v_6 = \left[\frac{s}{3} - s_1, \frac{w_{A1}}{2} + \left(\frac{s}{3} - s_1\right)\cot(\theta(x)), 0\right] \quad (11b)$$

$$v_7 = \left[\frac{s}{6} - s_2, \frac{-w_{B1}(x)}{2} + \left(\frac{s}{6} - s_2\right)\cot(\theta(x)), e - s_3\right] \quad (12a)$$

$$v_8 = \left[\frac{s}{6} - s_2, \frac{w_{B1}(x)}{2} + \left(\frac{s}{6} - s_2\right)\cot(\theta(x)), e - s_3\right] \quad (12b)$$

$$v_9 = \left[\frac{s}{6} - s_2, \frac{w_{B1}(x)}{2} + \left(\frac{s}{6} - s_2\right)\cot(\theta(x)), e + h_B(x) - s_3\right] \quad (12c)$$

$$v_{10} = \left[\frac{s}{6} - s_2, \frac{-w_{B1}(x)}{2} + \left(\frac{s}{6} - s_2\right)\cot(\theta(x)), e + h_B(x) - s_3\right] \quad (12d)$$

where s_1, s_2 and s_3 are parameters to adjust the translation region. Calculation of these parameters are not discussed in this study but they can be manually selected to fit the unit mesh to the real geometry.

3.3. Measurements on woven fabrics

In Fig.7 variable stiffness fabrics which are woven by 6k (2x3k) and 24k (2x12k) carbon fiber weft yarns and their close-up images are presented where the orientation of the weft yarns varies from 900 to 200 from left side to right side. Measured values of the height and the width of region-A and region-B at $\theta(x) = 90^o$and the cross-sectional area of the weft yarns of the 6k and 24k fabrics are presented in Table-1.

Table 1. Thickness variations of the variable stiffness woven fabrics.

Fabric	$h_{A,ref}$ $[mm]$	w_{A0} $[mm]$	$h_{B,ref}$ $[mm]$	w_{B0} $[mm]$	A $[mm^2]$
6k	1.22	0.45	0.86	0.64	0.55
24k	1.23	1.82	0.86	2.60	2.24

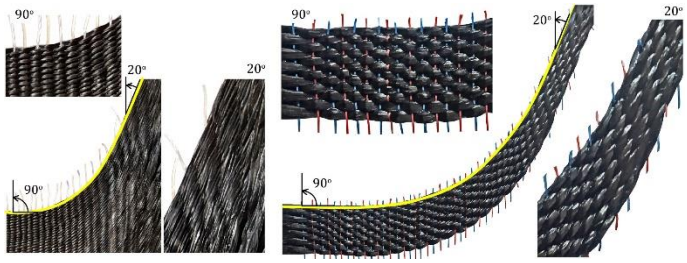

Fig.7. 6k and 24k variable stiffness woven fabrics in detail.

The width ratio C_1 is found as 0.7 by using values given in Table-1. The variation of the height and the width of A1 and B1 is calculated for the 6k and 24k fabrics by taking the shear factor C_2 as 0.5 and they are compared with experimental results in Fig.8. Additionally, the variation of A0, A1, B0 and B1 for 24k fabric is plotted in Fig.9.

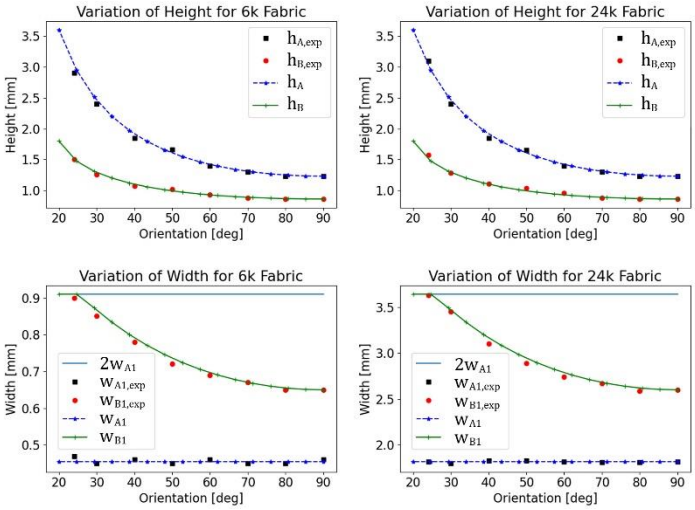

Fig.8. Variation of height and width of A1 and B1

From Fig.8 it is seen that the calculated values by using the developed model are consistent with the measured experimental values for region-A and region-B. It is also observed that the width values of the 6k and 24k fabrics are different while their height values are similar.

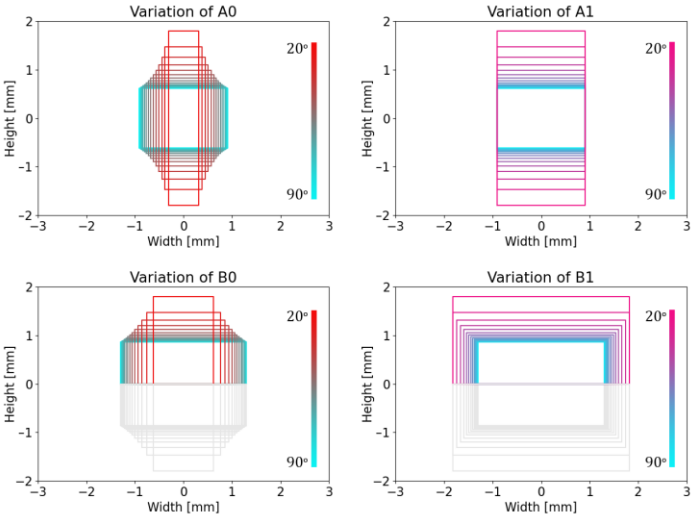

Fig.9. Variation of A0, A1, B0 and B1 for 24k fabric by orientation.

As the orientation decreases the height of A0 and B0, which are the cross sections perpendicular to the orientation, increases and inversly the width of A0 and B0 decreases as seen in Fig.9.

Also, as the orientation decreases the height of A1 increases while the width of A1 stays constant. The height and width of B1 both increases as the orientation decreases but when the width of B1 reaches at its limit value ($2w_{A1}$) it stays constant and the height of B1 starts to increase faster.

4. Conclusions and Recommendations

In this study a novel method to weave variable stiffness fabrics with curvilinear advanced fibers is presented. After basic working principle and the mechanism of the concept design is explained, an automated prototype loom is constructed. The use of the curved reeds in order to produce the curved shape of the fibers, requires longer strokes and extra rail supports for the reed and heddles compared to the ones used in the conventional looms. Many weaving experiments are realized on the prototype loom and it is seen that the desired curved shapes of the weft yarns can be achieved successfully by the method proposed.

It is observed that the weft yarns have two characteristic regions where the weft yarns behave differently. These two regions are named as region-A and region-B. When the weft yarns are pushed by the curved reed it is seen that the yarns at region-A only show shearing behavior while the yarns at region-B show both shearing and spreading behavior at the same time. Based on the behaviors of these two regions the section of the weft yarns between region A and B, which is repeating itself along the fabric, is simplified and modelled as a unit mesh. It is seen that variable stiffness woven fabrics can be successfully produced by the proposed method and the variation of the stiffness can be controlled by tailoring the curved path of the weft yarns. Since the concept design of the method presented is scalable, it is thought that this method can be applied in the mass production.

Unfortunately, because of Covid-19 pandemic experimental measurements of the stiffnesses of the woven fabrics are postponed and planned to be included in a further work.

5. Acknowledge

The authors would like to thank to Trakya University Research Fund for supporting the work presented, with a project reference TUBAP-2018/88.

References

Ashir, M., Nocke, A., & Cherif, C. (2020). Adaptive fiber-reinforced plastics based on open reed weaving and tailored fiber placement technology. *Textile Research Journal, 90*(9-10), 981-990.

August, Z., Ostrander, G., Michasiow, J., & Hauber, D. (2014). Recent developments in automated fiber placement of thermoplastic composites. *SAMPE J, 50*(2), 30-37.

Bai, J. (2013). *Advanced fibre-reinforced polymer (FRP) composites for structural applications*: Elsevier.

Blom, A. W., Setoodeh, S., Hol, J. M., & Gürdal, Z. (2008). Design of variable-stiffness conical shells for maximum fundamental eigenfrequency. *Computers & structures, 86*(9), 870-878.

Blom, A. W., Stickler, P. B., & Gürdal, Z. (2010). Optimization of a composite cylinder under bending by tailoring stiffness properties in circumferential direction. *Composites Part B: Engineering, 41*(2), 157-165.

Brooks, T. R., & Martins, J. R. R. A. (2018). On manufacturing constraints for tow-steered composite design optimization. *Composite structures, 204*, 548-559.

Campbell, F. C. (2010). *Structural composite materials*: ASM international.

Crothers, P., Drechsler, K., Feltin, D., Herszberg, I., & Kruckenberg, T. (1997). Tailored fibre placement to minimise stress concentrations. *Composites Part A: Applied Science and Manufacturing, 28*(7), 619-625.

Dirk, H. J. A. L., Ward, C., & Potter, K. D. (2012). The engineering aspects of automated prepreg layup: History, present and future. *Composites Part B: Engineering, 43*(3), 997-1009.

Gurdal, Z., & Olmedo, R. (1993). In-plane response of laminates with spatially varying fiber orientations-variable stiffness concept. *AIAA journal, 31*(4), 751-758.

Günay, M. G., & Timarci, T. (2017). Static analysis of thin-walled laminated composite closed-section beams with variable stiffness. *Composite structures, 182*, 67-78.

Günay, M. G., & Timarcı, T. (2019). Stresses in thin-walled composite laminated box-beams with curvilinear fibers: Antisymmetric and symmetric fiber paths. *Thin-Walled Structures, 138*, 170-182.

Gürdal, Z., Tatting, B. F., & Wu, C. (2008). Variable stiffness composite panels: effects of stiffness variation on the in-plane and buckling response. *Composites Part A: Applied Science and Manufacturing, 39*(5), 911-922.

Hyer, M. W., & Charette, R. (1991). Use of curvilinear fiber format in composite structure design. *AIAA journal, 29*(6), 1011-1015.

Hyer, M. W., & Lee, H. (1991). The use of curvilinear fiber format to improve buckling resistance of composite plates with central circular holes. *Composite structures, 18*(3), 239-261.

Jones, R. M. X. (1998). *Mechanics of composite materials*: CRC press.

Kim, B. C., Potter, K., & Weaver, P. M. (2012). Continuous tow shearing for manufacturing variable angle tow composites. *Composites Part A: Applied Science and Manufacturing, 43*(8), 1347-1356.

Kim, B. C., Weaver, P. M., & Potter, K. (2014). Manufacturing characteristics of the continuous tow shearing method for manufacturing of variable angle tow composites. *Composites Part A: Applied Science and Manufacturing, 61*, 141-151.

Leissa, A., & Martin, A. (1990). Vibration and buckling of rectangular composite plates with variable fiber spacing. *Composite structures, 14*(4), 339-357.

Lenz, C., Trinh, X. T., & Gries, T. (2016). Auslegung von Faser-verbundbauteilen auf Basis von Tailored Textiles. *Lightweight Design, 9*(3), 36-41.

Smith, F., & Grant, C. (2006). Automated processes for composite aircraft structure. *Industrial Robot: An International Journal*.

Zamani, Z., Haddadpour, H., & Ghazavi, M.-R. (2011). Curvilinear fiber optimization tools for design thin walled beams. *Thin-Walled Structures, 49*(3), 448-454.

Zhang, W., Liu, F., Lv, Y., & Ding, X. (2020). Modelling and layout design for an automated fibre placement mechanism. *Mechanism and Machine Theory, 144*, 103651.